A cadaveric porcine corneal wound model using semi-automated assessment

by

Orman Lawrence Snyder II

B.S., Kansas State University, 1974
DVM, Kansas State University, 1976

A REPORT

submitted in partial fulfillment of the requirements for the degree

MASTER OF SCIENCE

Department of Veterinary Biomedical Sciences
College of Veterinary Medicine

KANSAS STATE UNIVERSITY
Manhattan, Kansas

2020

Approved by:

Major Professor
Mark L. Weiss, Ph.D.

Copyright

Abstract

Corneal injuries constitute a major clinical problem in both human and veterinary medicine. Because of this, new methods to improve corneal healing are constantly being developed and tested for safety and efficacy. Historically, corneal injury models utilize rabbits to evaluate therapeutic or toxic compounds, e.g., the Draize test. Animal welfare concerns and the cruelty of live-animal testing have prompted the development of cadaveric corneal injury models. Cadaveric models using rabbits, chickens or pigs are preferred since these animals are slaughtered for food production and thus, intact eyes may be obtained with minimal ethical concerns. In comparison to rabbit and chicken, porcine corneas are anatomically and physiologically more similar to human corneas. For this reason, porcine corneas were tested here. The goal was to develop cadaveric cornea culture, corneal wounding, and assessment methods to enable standardized for preclinical evaluation of novel therapeutics. Two wounding methods were tested here: physical injury and chemical injury. Chemical injury using 0.5 M Sodium Hydroxide (NaOH) for 30 seconds applied using a 7.2 mm filter paper disk produced reproducible corneal epithelial damage. A semi-automated method for wound assessment was developed using a SpectraMax i3 plate reader to measure wound size following fluorescein application. Together, the data show that wound healing occurs for the first 24-48 h after injury and plate reader-based imaging documents wound size in a relatively unbiased manner. These methods lend themselves to testing novel therapeutic agents for safety and efficacy for preclinical evaluation.

Table of Contents

List of Figures

List of Tables

Acknowledgements

The author would like to thank his graduate committee, Drs. Santosh Aryal, Robert DeLong and. Mark Weiss for their assistance with my training. Dr. Weiss is also thanked for statistical evaluation and analysis, production of the 3-D printed mold for the corneal supports and computer expertise in developing software modifications for the SpectraMax i3 corneal wound analysis used in my thesis. The Banner Creek Facility of the Johnsonville Corp. and their staff (Donnie Merchant) are thanked for supplying tissues. Dr. Hong He and Adrienne Wright are thanked for helpful conversations, advice and technical support. Dr. Dan Boyle and Dr. Jessica Meekins were invaluable for information regarding corneal biology and their advice was greatly appreciated. Dr. Joan Murnane deserves a great deal of thanks for her encouragement to advance my career with continued education. The author thanks Ms. Rachael Madera for training and Dr. Jishu Shi for access to the SpectraMax i3. This study was supported by the State of Kansas to the Midwest Institute for Comparative Stem Cell Biotechnology.

A very big “Thank You!” to my wife, Jeanine, for her patience and support through this learning process.

Introduction

The cornea is a transparent tissue where light enters the eye and thus, it is important to vision. The cornea epithelium is the protective, exterior layer and consists of four to six layers of nonkeratinized, stratified squamous cells. In life, this epithelium is covered by a tear-film that smooths out surface irregularities, lubricates, and prevents drying. The epithelia tissue is continuously replaced by limbal stem cells located at the limbo-scleral junction which differentiate into basal cells, and basal cells differentiate into wing cells, and wing cells differentiate into squamous cells that form the superficial layers of the corneal surface [1,2]. Human corneal epithelial cells are sloughed continuously and have a lifespan of seven to ten days with centripetal replacement via proliferation, differentiation, and migration of limbal stem cells derivatives [2,3].

Currently in the United States, ≈8% of all human emergency room visits [4], and ≈4 - 6% of veterinary visits (OLS, personal observations at University Bird and Small Animal Clinic, 1984-2020) are due to corneal injuries. It is estimated that 20% of the US population will suffer some form of eye trauma during their lifetime [2,5]. Currently, over 10 million people worldwide are affected by corneal blindness [6]. In the US there are approximately 50,000 corneal transplants annually, with a significant short-term and long-term failure rate [6]. However corneal transplants are successful only when the limbal stem cells remain.

Corneal injuries are constantly exposed to the external environment. Although superficial corneal abrasions usually heal, rapid re-epithelialization is critical to preserve corneal transparency and vision before secondary infections become established. The “standard of care” consists of supportive therapy via eyedrops providing anti-drying agents that often contain

antibiotics, anti-inflammatory drugs, and topical anesthetics to the damaged surface [4]. Therefore non-steroidal anti-inflammatory drugs (NSAIDs) and topical anesthetics that depress the rate of corneal re-epithelization are contraindicated [4].

The clinical evaluation of corneal damage is subjective due to reliance on slit-lamp observation by experienced ophthalmologists or computer-assisted image analysis. Methods of assessment at referral ophthalmology centers include specialized imaging technologies such as Anterior Segment Optical Coherence Tomography (AS-OCT), Ultrasound Bio-microscopy, Corneal Epithelial 3D Mapping by Very High-frequency Digital Ultrasound, Ultra High Resolution Optical Coherence Tomography (UHR-OCT), or Confocal Microscopy [7-9]. Some of these methods, such as UHR-OCT, offer resolution of all corneal layers at nearly a histological level. Thus, they detail corneal wound healing at nearly cellular resolution. In contrast, clinical evaluation via fluorescein staining and slit-lamp examination or image analysis shows only the area of the wound, and does not provide detailed information about wound depth or epithelial regrowth [9-11]. While UHR-OCT systems are available for clinical research and *in vivo* assessment, they may not be useful for evaluation of cadaveric corneas *in vitro*, e.g., for preclinical testing of novel therapeutics.

Sodium fluorescein staining of cornea tissue has been used clinically for more than 100 years to evaluate cornea damage [12]. Fluorescein is a low molecular weight fluorescent dye with 400-500 nm excitation wavelength, and it easily diffuses into the cornea stroma after either loss of cornea epithelium barrier function (i.e., loss of tight junctions) or losses of superficial cornea epithelium cells due to physical or chemical damage [10]. Recent work indicates that fluorescein stain is taken up both by damaged cornea squamous cells and deeper stromal cells [10,13]. Importantly, fluorescein staining is used as a primary endpoint by the Food and Drug

Adminstration for efficacy testing of all new therapeutics [13]. Current model of corneal healing suggests that a single layer of basal limbal epithelial cells is pushed over the wound bed centripetally from the limbus by an increasing population pressure gradient to close the wound [1]. The cell movement rapidly covers the wound. The basal cells that have covered the wound differentiate to fill in the missing cell epithelial layers to eventually reform the cornea surface. In the mouse *in vivo* model used by Park et al. (2019), the corneal wound was covered with basal cell progeny in 24 hours and retain a small amount of fluorescein stain, but the cornea did not return to normal architecture for 4 weeks [1]. Normal barrier function of the corneal epithelium may be restored at the point of coverage of the wound by the basal cell layer but it retains dim fluorescein stain [10]. Other work indicates that innervation and insulin-like growth factor 1 play a role in corneal epithelial migration and recovery of barrier function after wounding [2,14]. We assumed that the extent of closure of the wound is directly correlated to the area of stain uptake. Therefore, throughout this thesis, we interchangeably use "fluorescein staining" for "cornea damage". Similarly, we defined "healing" as a significant decrease in the area stained by fluorescein realizing that the cornea has not returned to normal histology. We acknowledge that these represent indirect measures of cornea damage which should correlate with histopathology assessment.

We evaluated wounding and healing with 2 different ImageJ photogrammetry methods from photographs of fluorescein-stained corneas. Two dimensional photogrammetry is the science of reliable recording, measuring, and interpreting photographic images to obtain a defined area [15]. The ImageJ methods employed required manually setting the region of interest via thresholding of hue, saturation, and intensity or by manually outlining the wound margin. The subjective nature of these results prompted us to investigate a novel unbiased method to

measure fluorescein stain retention using a SpectraMax i3 plate reader. This method produces a semi-automated area measurement of corneal fluorescein staining.

There are many methods for porcine cornea culture in the literature [16-23]. Culture for 25 days or longer has been reported [18,19]. Wound healing has been reported to occur between 0 - 48 hours *in vitro* in rabbits [24], in 24 hours *in vitro* in mice [1] and in 24 - 72 hours *in vitro* in swine [25,26]. Based upon this time range for in vitro cornea wound healing, here, we sought to culture porcine corneas for up to 96 hours to evaluate first-intention wound healing.

The extent of the initial injury is a major factor in determining the progression of corneal healing [27,28], meaning that larger wounds are expected to heal more slowly than smaller wounds, and any wound that destroys the limbal stem cell population is unable to heal [2,6]. We considered what would be an appropriate amount of the surface to damage. The wounds evaluated by Park et al. (2019) were created by physical removal of the epithelium and were 2 mm in diameter (3.14 mm2) on mouse corneas. This corresponds to approximately 50% of the surface area. Park et al. (2019) found significant decrease in fluorescein staining in 8 hours with complete lack of staining in 24 hours *in vitro*. Here, we created a wound of 7.2 mm to 8 mm in diameter (41 - 50 mm2) in the porcine corneas, which corresponds to 18 - 21% of the cornea surface area [1]. Assuming the pig cornea heals at approximately the same rate as the mouse, we expected wound healing to occur over the 96-hour culture period. We found significant healing, as defined as significant decrease in fluorescein-stained area, after 24 - 72 hours here.

The mechanism of wounding impacts the healing rate, too, with superficial physical wounds healing more quickly than chemical wounds [26,28,29]. In addition, there is the challenge to produce consistent wounding. Both physical and chemical cornea wound methods were considered for use here [28,30,31]. For example, physical removal of the corneal epithelium via

scalpel blade or Algerbrush [20,24,31] and, chemical damage of the corneal epithelium by hydrochloric acid, sodium hydroxide, 20% methanol, or N-Heptanol solutions were considered [17,18,30,32]. Deeper blade wounds that extend through the basement membrane into the stroma have been shown to result in elevated stromal remodeling with replenishment of the keratinocytes from the areas adjacent to the area of injury, resulting in delayed healing and possible fibrotic changes [2]. Here, the application of 0.5 M NaOH via paper disk produced the most controlled and consistent method to damage the cornea epithelium when compared to the other wounding methods evaluated.

Methodology

Tissue Collection and Processing

Institutional animal care and use committee (IACUC) reviewed and approved this research (IACUC protocol #4185). The eyes were obtained from female pigs (mixed breed commercial production sows) weighing 300 to 400 pounds at slaughter. The pigs were processed for food production (n=134) and the eyes were harvested within 15 minutes after death by the staff at the Banner Creek Processing Plant of Johnsonville, LLC (Holton, KS). The experimental protocol is shown schematically in Figure 1. The intact eyes were immediately rinsed with cold, sterile Sorenson's Phosphate Buffered Saline (PBS, 50 mM buffer, 0.9% NaCl, pH 7.4-7.6) with 1% Antibiotic/Antimycotic (Gibco, Catalog No. 15240062), placed into cold PBS and transported on ice to the laboratory. On arrival at the laboratory, the eyes were stained with 0.5% Lissamine Green B (AlfaAesar, Cat. #190100250) in sterile water to evaluate corneal surface damage [33], and eyes with a damaged cornea were discarded. The healthy corneas were photographed *in situ* after staining (see Figure 2A), and adnexa (excess tissue surrounding the eye globe) was dissected and discarded. To sanitize the eyes, they were placed in a freshly prepared room temperature 0.75% povidone-iodine solution (Aplicare, NDC-5238-1905-9) for 2 minutes [34] and then transferred without rinsing into 3 volumes of room temperature Dulbecco's Phosphate Buffered Saline (DPBS, Sigma, Cat#D8537-500ml) for 2 minutes. The corneas were then wounded prior to dissection from the eyeball.

Figure 1

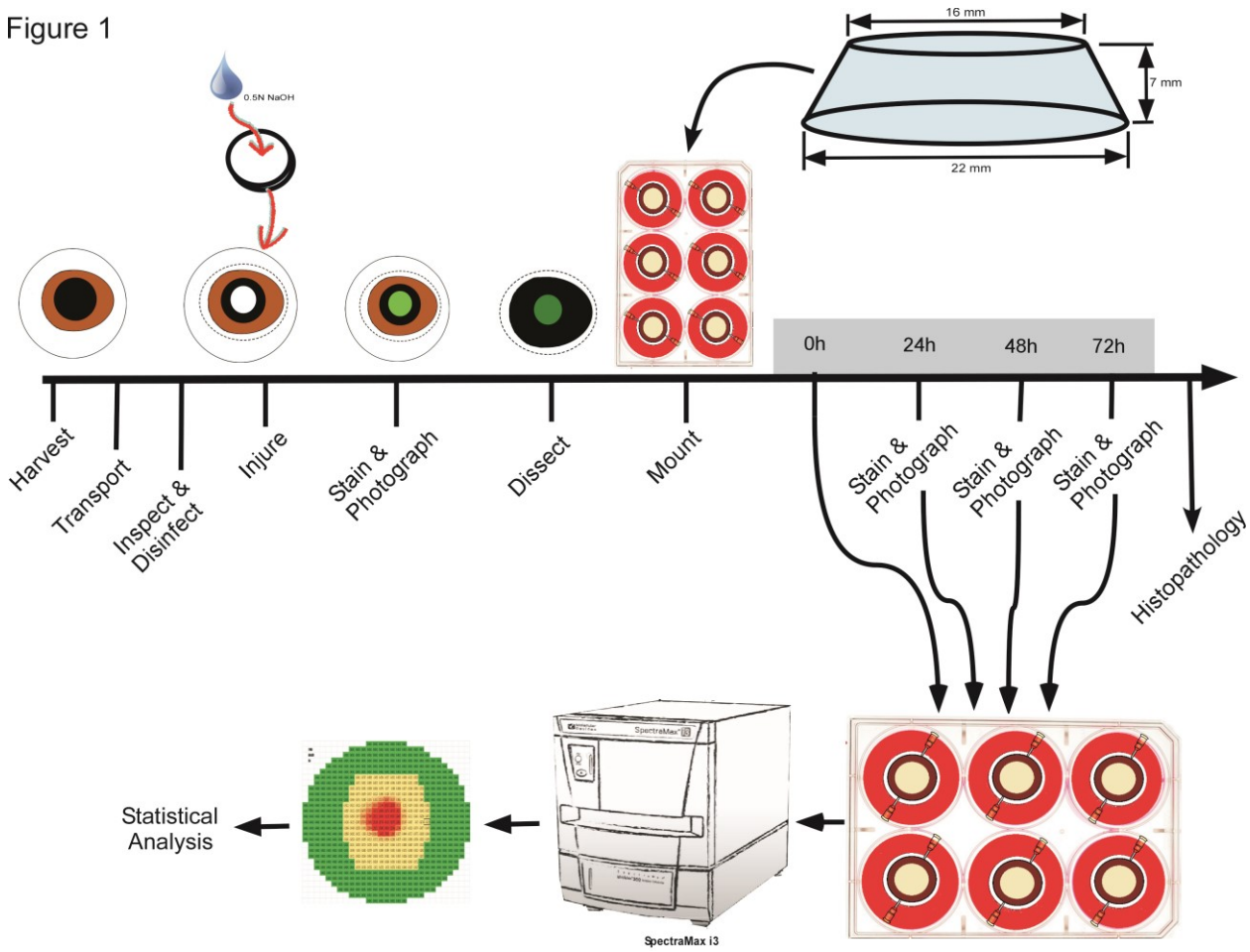

Figure 1. Schematic of swine corneal wound model experiment. Pigs were sacrificed at the Banner Creek food production plant of Johnsonville, LLC. Plant employees removing the eyes for further processing (HARVEST). The globes were rinsed and placed in cold physiologic buffered saline solution within a cooler for transportation to the laboratory (TRANSPORT). Once in the laboratory, the eyes were inspected by lissamine staining for damage and undamaged eyes were bathed in dilute povidone-iodine solution for decontamination (INSPECT & DISINFECT). Globes were mounted on a stage and the cornea wounded, for example, by applying a paper disk soaked with sodium hydroxide to the center of the cornea, followed by rinsing (INJURE). The wound was documented, prior to dissection from the globe (Stain & Photograph). The cornea was dissected 2 mm distal to the corneoscleral junction (DISSECT) and pinned on a silicone stage (see inset for dimensions) within a 6 well tissue culture plate (MOUNT). The medium was added, and the plate was placed on a tilted rotating stage to swirl medium across the corneal surface within a tissue culture incubator. At fixed times after wounding, 0, 24, 48 and 72 hours, the plate was removed, and the wound was evaluated following fluorescein staining by photography and imaging within the SpectraMax i3. The wound area was quantified in the photographs using ImageJ or determined spectrographically by SpectraMax i3 scanning. The changes in the determined wound size was statistically analyzed.

Cornea Isolation and Culture

Following wounding, the corneas were dissected for culture. Using sterile technique, corneas and surrounding sclera 3-5 mm distal to the corneoscleral junction (limbal rim) were removed and a fiducial mark was made to maintain anatomical orientation (see Figure 2D). The uvea was bluntly dissected from the lens and pupil. The isolated cornea was rinsed with DPBS and pinned to a custom-molded silicone support (described below) in a 6-well tissue culture plate (CytoOne, 6 well, Cat. #CC7682-7506) using 27-gauge x ½" needles (Monoject Cat. #8881250362) positioned diametrically through the sclera (see Figure 1).

The corneal surface was kept moist with sterile Pig Cornea Medium (PCM) consisting of Dulbecco's Modified Eagles Medium (DMEM) / F-12 (1:1) (Gibco, Cat. #11330-032) supplemented with 10% fetal bovine serum (HyClone, GE Healthcare Life Sciences, Cat. #SH3007103), 1% antibiotic-antimycotic (Gibco, Cat. #15240096), 1% Glutamax (Gibco, Cat. #35-050-061), 0.01% Dextran 40 (AlfaAesar, Cat. # J-63690) and 0.025% Chondroitin Sulfate (AlfaAesar, Cat. #J66156). Sterile distilled water was placed into the space between the culture wells to stabilize humidity and temperature during incubation in a Nuaire AutoFlow 4950 incubator at 37°C, 5% CO_2, 90% humidity. The plates were axially rocked (GyroMini, LabNet Nutating Mixer, Cat #50500) to moisten the superficial surface regularly without submersing the cornea in PCM.

Figure 2

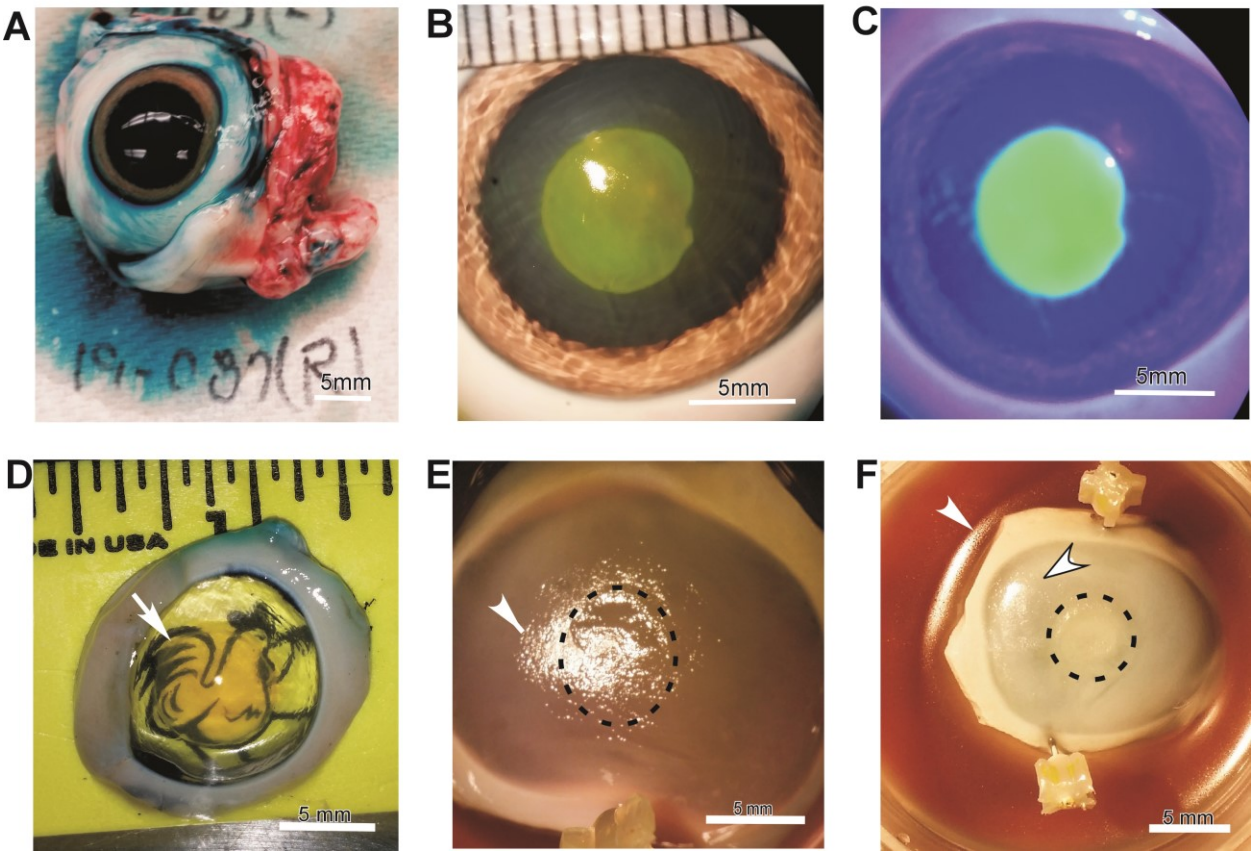

Figure 2**.** Gross observation of cornea. A. Whole globes were evaluated by lissamine staining (blue stain) to exclude corneas that were damaged during Harvest and Transport prior to the experiment. Note the glistening appearance of the fresh healthy cornea. B. After wounding, fluorescein was taken up in the wounded area. Note that cornea was damaged by the application of a paper disk soaked in 0.5N sodium hydroxide for thirty seconds. Note the central location of the damage and its margins as demonstrated by fluorescein staining. Note also the slight granular appearance of the damaged surface (look at the bright reflected area). C. Same wounded cornea as shown in B under fluorescence observation. D. Cornea immediately after dissection from the globe. Note that the wounded area and wound margins are defined (arrow). Note that the wounded area was less transparent than the adjacent unwounded area. E. Cornea 72 hours after culture. Note the wounded area is within the dotted line, and that the surface of the cornea is no longer glossy, with a textured appearance (arrowhead). F. Cornea 96 hours after culture. Note that the cornea has lost transparency and has a more pronounced textured appearance (black-outlined arrowhead). Ulceration was also observed. The culture media has an oily sheen indicating tissue coagulative necrosis (black outlined arrowhead). The dotted line indicates the wounded area. Note that the wounded area was less sharply defined. The calibration bar is 5 mm.

Silicone Support Production

Clear silicone supports were cast using 3D printed ABS molds. The support dimensions are shown in the inset of Figure 1, and the *.stl file to print these parts is available from the NIH 3D print exchange (https://3dprint.nih.gov/discover/3dpx-014177). To cast, a mold release agent was applied per the manufacturer's instructions (CRC Food Grade Mold Release), and each mold was filled with Sylgard 184 Silicone Elastomer (Kit #ET033568). The silicone was degassed under vacuum for 20 minutes at room temperature, and then cured at 50°C for a minimum of 4-6 hours. Silicon supports were removed from the mold, washed thoroughly and rinsed with distilled water and dried. The supports were then attached to each well of a 6-well plate with fresh Sylgard 184. The adhesive silicone was cured at 50°C for > 12 hours, cooled and stored for > 7 days at room temperature before use. Plates were disinfected prior to and after their use. To disinfect, the wells were rinsed twice with hot tap water followed by soaking in hot tap water for 5 minutes with 5 changes. Plates were then soaked in freshly prepared tissue culture detergent (MP Biomedicals, 7X Detergent, 1ml detergent in 100ml tap water) for 30 minutes. Plates were rinsed twice in hot tap water and then soaked in hot tap water for 5 minutes with 5 changes. Plates were then soaked in a freshly prepared 5% bleach (5000 PPM Sodium Hypochlorite, Clorox bleach) in tap water for 30 minutes. Plates were rinsed twice in cold tap water and then soaked in cold tap water for 5 minutes with 5 changes. Plates were then soaked in distilled water for 5 minutes with 3 changes. Plates were then airdried inside a sterile class IV biological safety cabinet (BSC, Baker Steril-Guard III) while exposed to UV illumination. Without removing the plates from the BSC, they were sprayed with 70% ethyl alcohol with 5 minutes of contact time prior to being airdried again in the BSC with UV illumination. At this

point, the plates were deemed disinfected and handled using aseptic technique. The lids were replaced, and the plates were wrapped in plastic wrap (Saran Wrap) prior to labeling and removal from the BSC for storage.

Fluorescein Staining

Corneas were stained prior to removal from globes using I-Glo Fluorescein strips (JorVet 1 mg/strip, Lot #OUF180802) for 15 seconds, twice rinsed with 37 ˚C sterile Dulbecco's Phosphate Buffered Saline (DPBS; Sigma, Cat # D8537), and photographed using a 13-megapixel camera (Samsung – SM-N900A cell phone) mounted on a Wild M-10 microscope using near-vertical illumination. A ruler was used to scale the photographs. Photographs were taken with both white-light (TechniQuip Corp, 150W 3200 CCT halogen fiberoptic illuminator, model number FOI-150) and with light filtered using a Wratten 47-B filter (provides 400-500nm wavelength light, see Figure 2B-C)

Evaluation of Cornea Wounding Methods

Four methods of wounding were tested in pilot experiments to determine a uniform, predictable corneal epithelial wound model. Two of these methods and controls are presented here with the others provided in the supplemental information.

Prior to removal of the cornea from the globe, regardless of wounding method, photographs were taken next to a ruler to calibrate the image. The NIH ImageJ linear measurement tool was used to determine the major and minor axis of the porcine cornea [35]. The minor axis measurement was used to adjust for magnification differences in subsequent photographs of individual corneas. Settings of the illumination and orientation of the cornea were consistent for every image. Images were retaken following staining and media replacement at 24-hour intervals after wounding.

-Blade Debridement Injury

The cornea was scored with a circular blade and an 8 mm diameter (50 mm2) wound was made through the epithelium to approximately the depth of the epithelial basement membrane by scraping with a sterile scalpel blade. The wound was documented by fluorescein staining and photographs were taken within 15 minutes of corneal staining. The corneas were excised and pinned on silicone supports in the 6-well plates. The plates were sealed with optically clear sealing tape (iCycler iQ Optical Tape, Cat. #2239444) and imaged with the SpectraMax i3.

-0.5N Sodium Hydroxide (NaOH) Injury

In pilot work, we found that different severity of wounding could be created by first adding 15 µl 0.5N NaOH to a 7.2 mm diameter Whatman #2 filter disk and applying the disk to the cornea for 15-, 30- or 60-seconds. After removing the disk, the corneal was rinsed repeatedly. In the work described here, the 30-second application of 0.5N NaOH was used. Wounds were fluorescein-stained after injury to document the damaged area at time 0. Photographs were taken within 15 minutes of staining. The corneas were excised and placed on silicone supports in the 6-well plates prior to being imaged with the SpectraMax.

-Uninjured Controls

Ten porcine eyes were processed in the same manner as those used for chemical wounding except 15 µl of sterile DPBS was added to the filter disks and the disks were left in place for 30 seconds. Corneas were stained with fluorescein and photographs were taken within 15 minutes of staining to document the damaged area. The corneas and limbal rims were excised and placed on supports in the 6-well plates, and the plates were sealed with optically clear sealing tape and imaged with the SpectraMax i3, prior to being placed on the rotating platform in the incubator (as detailed in corneal culture and isolation).

Photogrammetric-Evaluation of Corneal Healing

The wound area was determined from digital photographs taken with Wratten 47-B filtered light, using 2 methods after being imported into ImageJ [35]. The Color Threshold tool requires independent adjustment of color hue, brightness, and saturation values for each image. A representative corneal wound was used to set the color hue value to (83/145), the brightness value to (139/255), and the saturation value to (0/255). Next, the pixels of the image that fit the color, intensity, and saturation levels were automatically identified and the area of interest was measured. The Outline Area tool allows the area of fluorescein staining identified by the user's manually drawn region of interest using a mouse-driven cursor. The wound area determined by both methods was recorded.

Spectrophotometric Evaluation of Corneal Healing

SpectraMax i3 (Molecular Devices, s/n: 353701379, Softmax Pro 7.1 for Windows 10 software) was prewarmed to 35°C for 15 minutes prior to imaging. The instrument scanned the entire well of a 6 well plate in the fluorescence intensity mode, each well received 3 flashes per read, 614 pixel reads/well, 480 nm excitation, and 530 nm emission. At 24-hour intervals the plate was removed from the incubator, and in the BSC, the media was removed, the cornea rinsed with warmed sterile DPBS and re-stained with I-Glo Fluorescein. Following staining, the cornea was rinsed with 2 ml of warmed DPBS, the well was aspirated and an additional 1 ml of warmed DPBS was flushed over the cornea. This final rinse was then aspirated before 3 ml of fresh PCM media was placed in the well. The wells were sealed with optically clear sealing tape, then placed in a heated, insulated container for transport to the SpectraMax i3. The plate was placed in the pre-warmed SpectraMax i3 chamber and scanned. After imaging, the plate

was returned to the BSC where the optical tape was replaced with the plate lid and the plate was put back on the rocking platform within the incubator.

Data from the SpectraMax i3 was analyzed from the central area of each well, which represented the location of the cornea and scleral ring being scanned (see Figure 1C). The Relative Fluorescence Units (RFU) generated during each scan reflect a non-adjustable photo multiplier tube (PMT) gain that automatically normalizes data to fit a linear curve (personal communication: Hongming Zhu, PhD Technical Support Supervisor, Plate Reader, Liquid Handling, and HTS applications, Molecular Devices (LLC).

The RFU data was post-processed by Z-score normalization using a custom Excel macro that parsed these values into 4 thresholds of intensity (> +1.3SD, > +1.7SD, > +2.5SD, > +3.5SD) and generated a color-coded picture element map of regions that exceeded the threshold, and calculated total wounded area that exceeded each threshold. Examples of these maps are shown in Figure 5.

Cornea Histopathology

Fiducial marks (sutures) were placed in the scleral rim and the cornea was fixed in 10% neutral buffered formalin for at least 48 hours. Corneas were submitted to Kansas State Veterinary Diagnostic Laboratory's Histopathology Service for paraffin embedding and Hematoxylin & Eosin staining. Slides containing three 10 µm sections of each cornea were taken: 1) through the central ulcerated area, 2) medial mid-corneal area, 3) lateral mid-corneal area. Slides were masked prior to being evaluated by Dr. Giselle Cino, ACVP board-certified veterinary pathologist and one of the authors (OLS), independently using modified standard measures (see Table 1) based on previously established criteria [36]. The following three criteria were evaluated using a 0 – 4-point linear scale: 1) Extent of ulceration, 2) Quality of Epithelium,

3) Extent of Inflammation, Edema, Degeneration. The total score (0 to 12) comprised the Global Histology Score (GHS). GHS scores from the two observers were averaged. A GHS of 3 or less was considered healthy or healed. Note that two of the three criteria evaluate epithelium.

Table 1. Criteria for histopathological evaluation of corneas.

Ulceration/Erosion	**Quality of Epithelium**	**Inflammation/Edema/ Degeneration**
0 = None	0 = Normal	0 = None
1 = <25% Surface	1 = Focal Degeneration Metaplasia	1 = Small Numbers/Mild/ Mild Degeneration
2 = 25 – 50% Surface	2 = Regional Degeneration/ Metaplasia	2 = Moderate Numbers, Moderate/Moderate Degen.
3 = 50 75% Surface	3 = Global Degeneration/ Metaplasia	3 = Moderate Global – All Parameters
4 = >75% Surface	4 = Complete Sloughing	4 = Obliteration of Stroma

Statistics

Prior to the analysis, the analysis of variance (ANOVA) assumptions were checked. If assumptions were met, ANOVA was performed, and significant main effects or interactions were identified. Pre-planned comparisons were performed after applying Bonferroni's correction. Those data are presented as mean (average) plus/minus one standard deviation (SD). If ANOVA assumptions were not met, the Kruskal-Wallis non-parametric analysis of variance on ranks was used to evaluate the main effects. In this case, post hoc pre-planned comparisons were evaluated using Tukey's honest significance test. Those data are presented in box and whisker plots showing median and 25th and 75th percentile in the box and whiskers showing 10th and 90th percentile with potential outliers indicated by circles. In text, the data are presented as mean ± one SD unless stated otherwise. The graphs were created using SigmaPlot (Systat Software, Inc, version 14.0, build 14.0.3.192) and were saved as EMF files. The EMF graphs were imported

into Canvas GFX, Inc's Canvas X (version 15 or version 19, Build 333) for final production. In all cases $p < 0.05$ was considered "significant" in two-tailed testing.

Results

Development of Porcine Cadaveric Corneal Model

An experimental timeline is shown schematically in Figure 1. For the present work, 163 globes were obtained over a period of 16 months, and 134 uninjured, intact porcine eyeballs were used. Upon receiving the material in the laboratory, the cornea was flexible and transparent with a smooth, glossy surface (see Figure 2A). As shown in Figure 2B and C, both chemical or physical injuries resulted in a loss of the glistening smooth surface and a granular or textured appearance to the injured area. Injury by physical or chemical means increased the uptake of fluorescein in the wounded area. After dissection, the wounded corneas are still transparent and the fluorescein-stained area was visible after pinning it to the silicone base (see Figure 2D). The glossy appearance of the unwounded areas of the cornea persisted for 24 to 72 hours. As shown in Figure 2E, the cornea loses transparency over time and the entire corneal surface began to exhibit a granular texture. At 72 to 96 hours of culture, many of the preparations become flaccid and the corneas became opaque and edematous. At this time, the culture media showed acidification (yellow tint) and surface film between media changes (see Figure 2F). We checked the medium for the presence of bacterial contamination and no evidence of bacteria was found. The media acidification and tissue flaccidity suggest necrosis.

Assessment of Cornea Wounding Methods

Two methods, e.g., blade debridement (blade) or chemical injury using 30-second exposure to 0.5M NaOH are presented.

-Blade

Scraping the surface of the cornea was inconsistent, and removal of the corneal epithelium without complete or partial removal of the basement membrane proved to be difficult. Aggressive scraping increased uniformity, but the wound was extended through the basement membrane and into the stroma as noted in histopathology.

-Chemical

Both 2N HCl and 99% N-Heptanol were used as chemical wounding agents in pilot experiments, and those results are shown in the Supplemental Materials. Here, injuries produced by 0.5N sodium hydroxide (NaOH) for 30 seconds are shown. After removing the sodium hydroxide- soaked disk and rinsing the corneal surface, the wounded area was visible (see Figure 2D) and uniform fluorescein staining was visible within the wounded area.

-Control Wounds

A non-chemical injured control was prepared in the same manner as the chemical wound, but used a paper disk soaked in sterile DPS. Control procedure produced diffuse fluorescein staining that persisted through the culture period. The control wounds were only evaluated with the SpectraMax i3.

-Measurement Methods

As shown in Figure 3, we estimated wound size using three methods: ImageJ Color Threshold, ImageJ Outline, and SpectraMax i3 at time 0, and compared the wounded area to the measured injury in the intact globe (Intact globe). For the blade injury, 3 corneas were evaluated, and no differences were observed between methods (Figure 3A). For chemical injury, 47 corneas were compared at time 0 (Figure 3B). The ImageJ Color Threshold measurements were significantly smaller than the intact globe and showed the largest variation. The ImageJ Outline

method also measured a significantly smaller wound than the intact globe and showed less variation than the ImageJ Color Threshold method. In contrast, the SpectraMax i3 method area assessment was not different from that measured in the intact globe and were within 5% (39-43 mm^2) of the area of the paper disk (7.2 mm diameter, 40.7 mm^2).

Figure 3

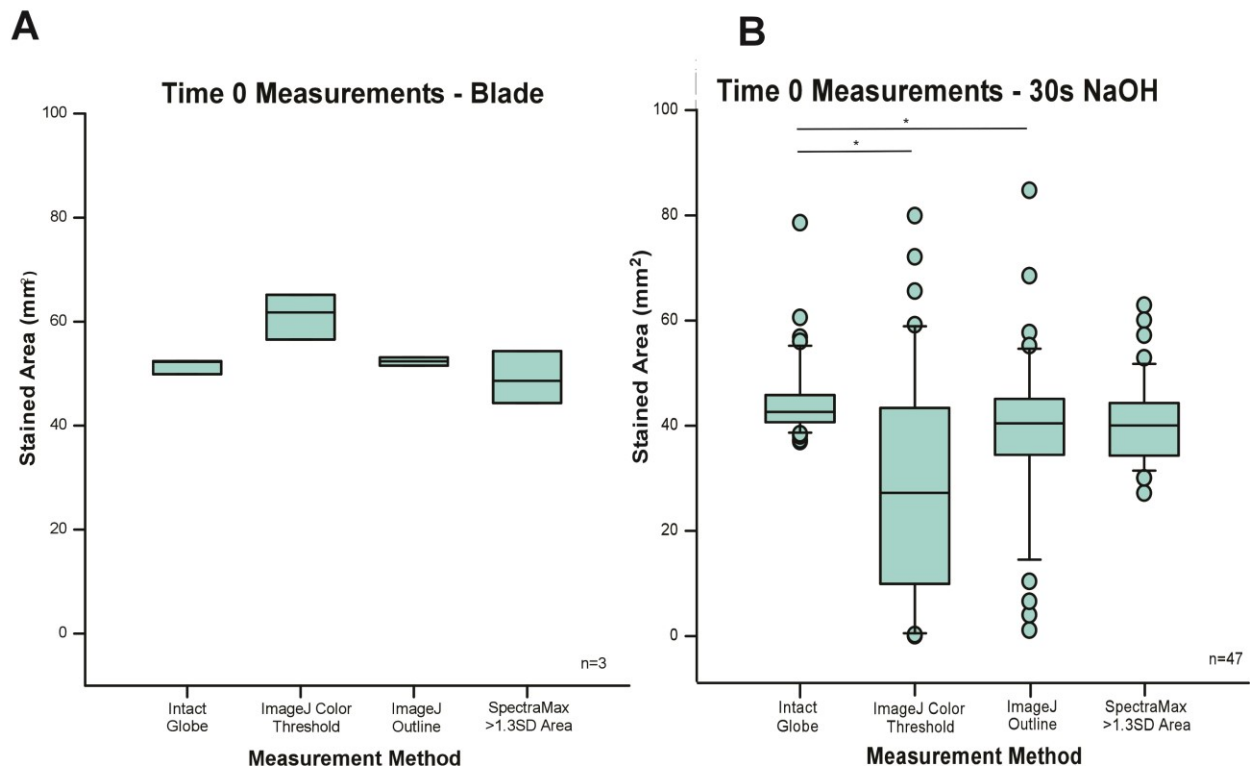

Figure 3. Wound size at time zero comparing four measurement methods. A. Blade injury (n=3). B. Chemical injury (n=47). The wound size (area) was estimated using a calibrated measurement of the wounded area from photographs of the fluorescein-stained area in the intact globe (Measured). This value was compared to measurements made after dissection with color thresholding measurement (ImageJ Color Threshold), outlining the wound (ImageJ Outline), or obtained from the area measured using the SpectraMax i3 of the staining > + 1.3 SD from the Z-transformed intensity (SpectraMax >+ 1.3 SD). Note that the ImageJ Color Threshold method tended to produce the largest variation of the wound size, followed by the ImageJ Outline method. Note that the SpectraMax estimate was not significantly different from the Measured area. Three cases were measured for physical injury and forty-seven cases were measured for chemical injury. Box and whisker plots with boxes indicating the 25th and 75th percentile and

median, and whiskers indicating 10^{th} and 90^{th} percentile. Dots indicate potential outlier observations (outside the 10^{th} to 90^{th} percentile range). * indicates $p < 0.05$ two tailed.

-Evidence of Wound Healing in Cultured Cornea

Figure 4 shows the comparison of the 3 measurement methods over the experimental time course of 0 - 72 hours, for blade injury (panel A) or for chemical injury (panel B). Both blade and chemical injuries showed a similar trend, and that indicate wound healing, e.g., a reduction of the area of the fluorescein staining, regardless of the measurement method over 48 - 72 hours of culture. Due to the low sample size, there was no significant difference in wound healing after blade injury. In contrast, chemical injuries showed significant wound healing when measured by SpectraMax i3 (left) or ImageJ Color Threshold (middle panel). Specifically, a significant decrease in the wound area was seen at 24 hours (ImageJ Color Threshold), or at 48 hours (SpectraMax i3) after wounding. The ImageJ Outline method was unable to detect significant changes in stained area. The standardized effect size (Cohen's d) of each method was analyzed to compare the initial 24 hours of culture 0 – 24 hours) to the final 24 hours of culture (48 – 72 hours). The SpectraMax i3 showed a standardized effect size of 0.9, and the ImageJ Color Threshold showed an effect size of 0.2.

Figure 4

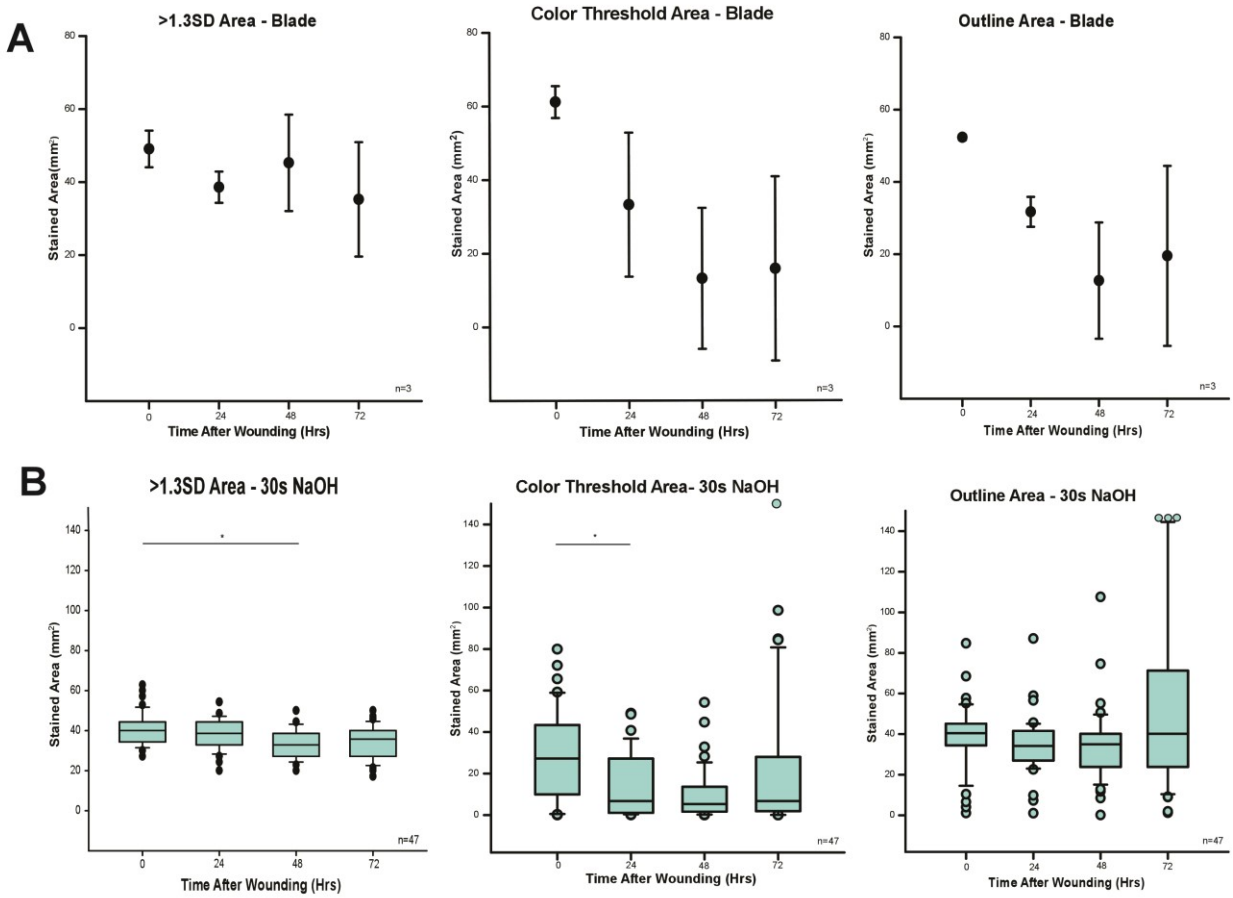

Figure 4. Decreases in the cornea fluorescein staining area over time indicates wound healing. A. Blade injury (n=3). Wound healing was suggested by a trend in the fluorescein-stained area over time regardless of whether it was measured by SpectraMax i3 (left), ImageJ Color Threshold, or ImageJ Outline methods. B. Chemical injury (n=47). (Left) When using the SpectraMax i3 (> + 1.3 SD Area), a statistically significant decrease in the staining area was observed at 48 hours. In contrast, using the ImageJ Color Threshold method (middle panel), a significant decrease in staining area was detected at 24 hours. The ImageJ Outline method (right panel) was unable to detect changes in wound area, but a trend indicated a decrease in the stained area over time. * indicates $p < 0.05$ two tailed.

Data collected via the SpectraMax i3 was in Relative Fluorescence Units (RFUs) of fluorescein staining with 614 independent readings collected per well map. An Excel macro was written to Z-transform the RFU per well. As shown in Figure 5, the Z-scaled RFUs were organized into a well map and color-coded such that values < +1.3 SDs were colored Green,

values between > +1.3SD and < +2.5SD were colored Blue, values between > +2.5SD and < +3.5SD were colored Yellow, and values over > +3.5SD were colored Red. The right panels of figure 5 plots the area represented in > +1.3SD, > +2.5SD and > +3.5SD Z-transformed values (top to bottom, respectively). In Figure 5A, control corneas (n=11) had no overt or gross pattern of fluorescein staining. Stain uptake was found at the periphery of the cornea (black line), perhaps due to damage during the initial dissection, due to the application of the paper disk, or due to mounting the tissue. In Figure 5B, blade-injured corneas showed wounding at time zero and healing over the 72 hours of culture, indicated by the decrease in fluorescein-stained area. The area graphs in the right panel show a reduction in the fluorescein-stained areas in the > +1.3SD and > +2.5SD graphs over time. In Figure 5C, 30-second exposure to NaOH (chemical injury) shows fluorescein staining > +2.5SD graph at time zero, and a gradual and consistent reduction of fluorescein stain area over time. The significant reduction in the stained area is considered to reflect wound healing after 48 hours of culture.

Figure 5 - A

Uninjured Control

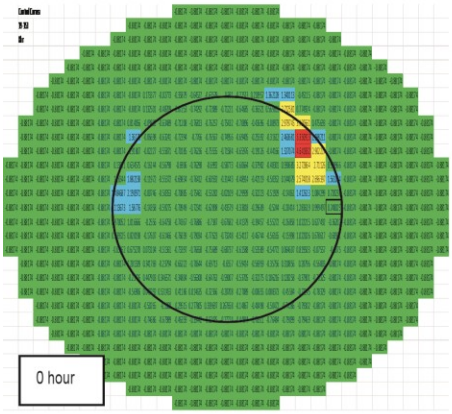

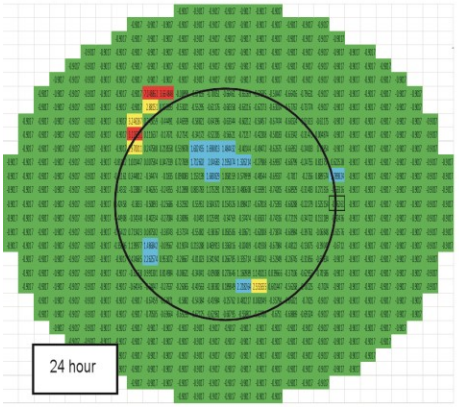

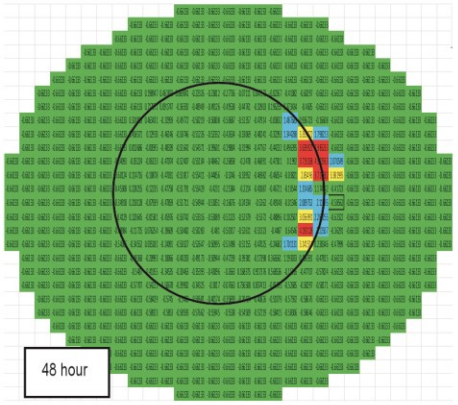

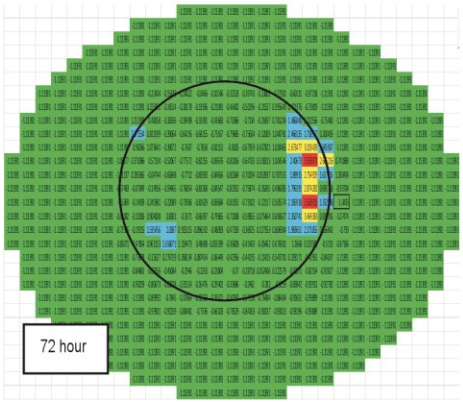

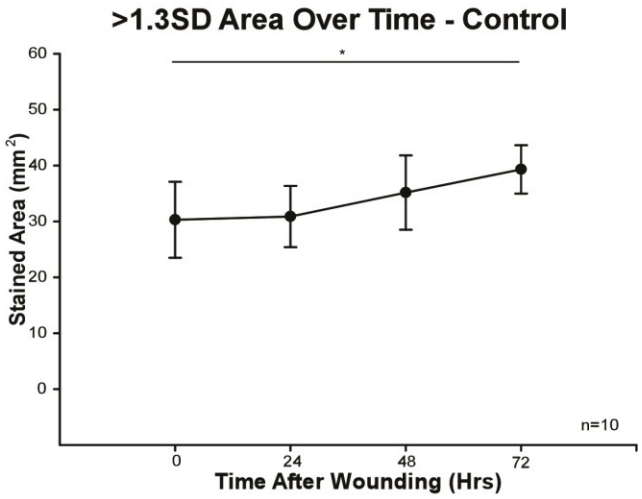

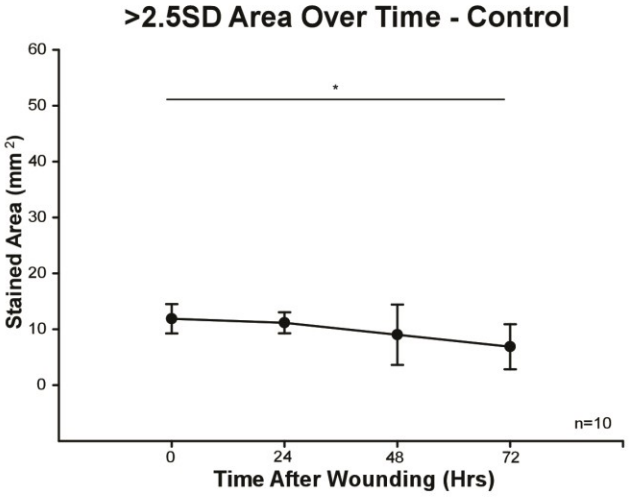

Figure 5 - B

Blade Injury

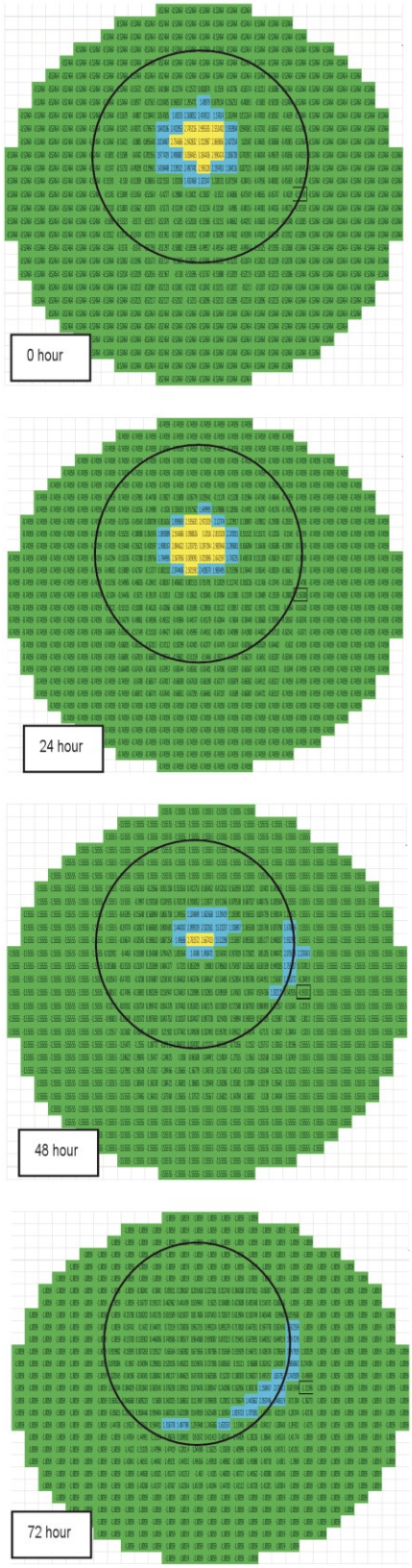

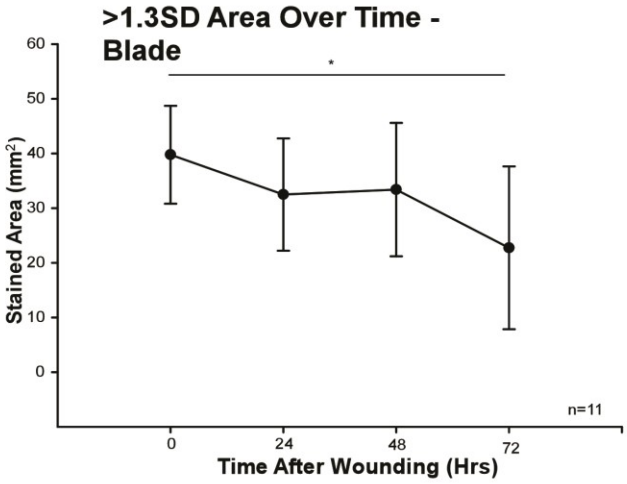

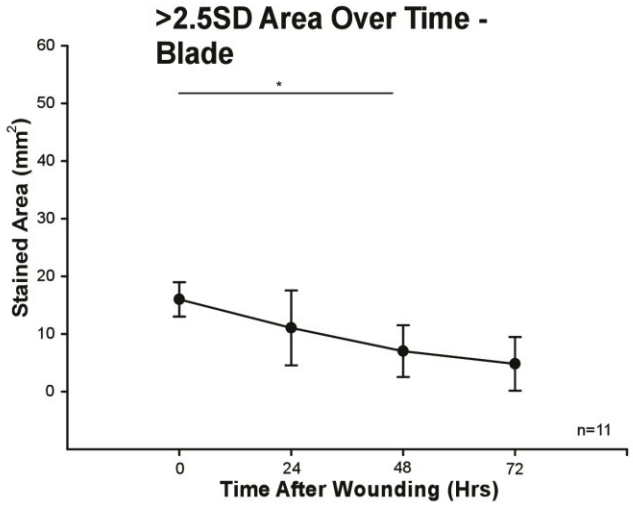

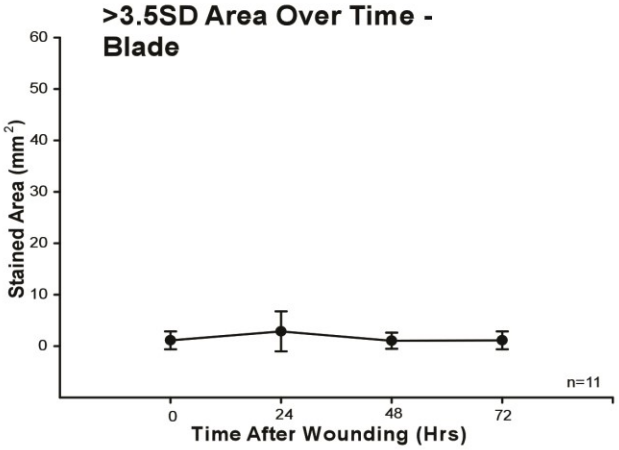

Figure 5 - C

NaOH Injury

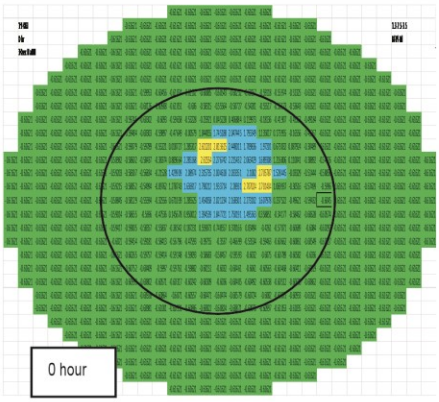

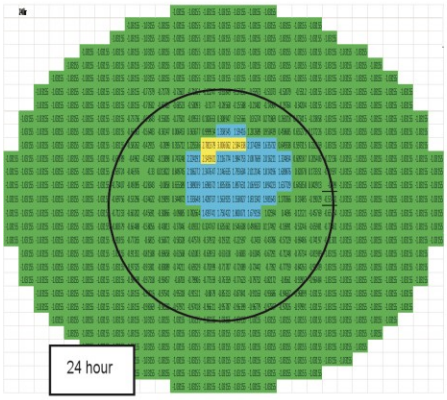

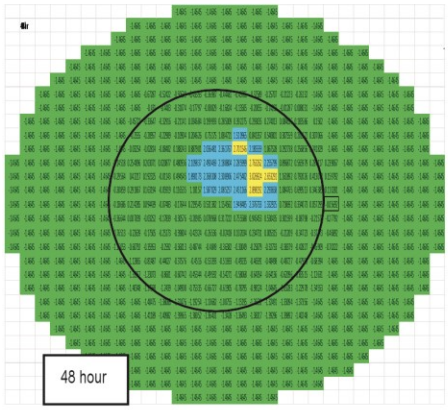

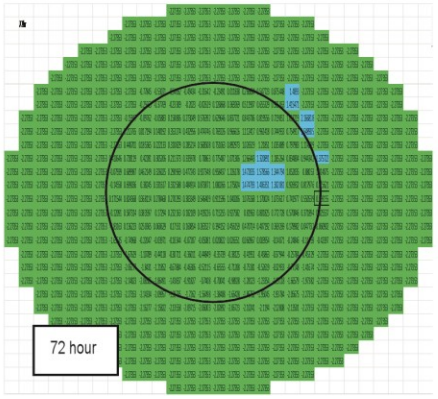

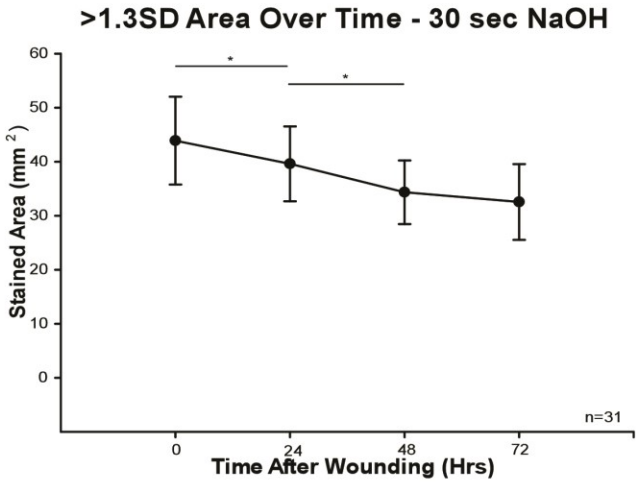

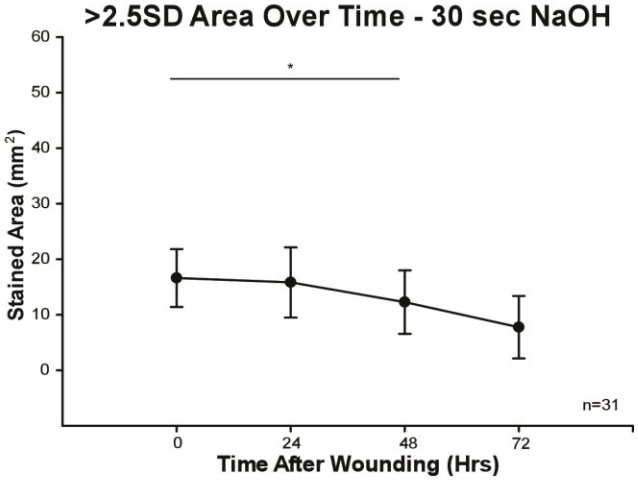

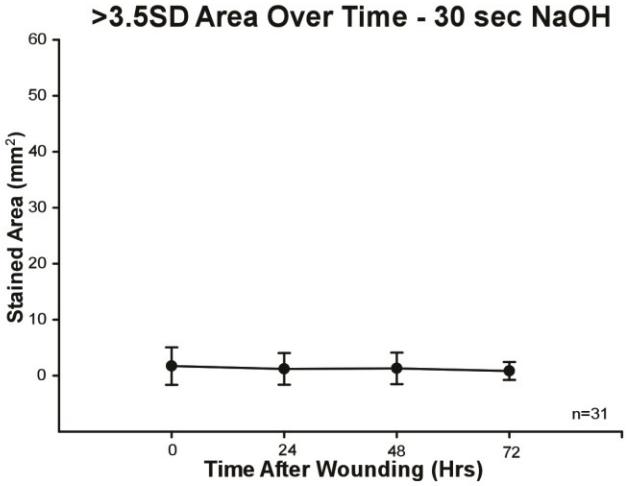

Figure 5**.** Semi-automated fluorescein-stained area assessment using the SpectraMax i3. The SpectraMax i3 digitizes fluorescent images that are scaled to relative fluorescence units (RFUs). Therefore, to compare images of the same cornea over time, the RFU were normalized using a Z-transformation, and the stained area was encoded by capturing the pixel elements that fall > + 1.3 standard deviations from the mean. To illustrate that here, on the left are example color-coded well plate images (green < + 1.3 SD, blue > + 1.3 and < + 2.5 SD, yellow > + 2.5 and < + 3.5 SD, and red > + 3.5 SD) versus time in culture (time 0, 24, 48 and 72 hours). Note the location of the cornea within the well is indicated by a black circle. On the right, the area corresponding to the normalized RFUs are plotted versus time in culture. A. HEALTHY control corneas. The healthy cornea does not show a consistent pattern of fluorescein staining. The > + 1.3 SD area tended to increase over the 72-hour culture period and the area became significantly different from time 0 at 72 hours. In contrast, the > + 2.5 SD area tended to decrease over the 72-hour culture period and became significantly different from time 0 at 72 hours. B. BLADE INJURY. The blade injury showed decreased fluorescein-stained area consistent with healing over the 72-hour culture period. This pattern was consistent in the > + 1.3 SD and > + 2.5 SD datasets. Thus, a decrease in fluorescein-stained area was observed over the 72-hour experiment. C. CHEMICAL INJURY. After sodium hydroxide-induced injury, a decrease in fluorescein-stained area was consistent with healing over 72-hours. Stained area decreased in both the > + 1.3 SD and the > + 2.5 SD datasets. Significant decreases in fluorescein-stained area was observed after 24 hours. Stained area continued to decrease between 24 hours and 48 hours observations, suggesting further significant healing. Data presented as means ± SD. * indicates $p < 0.05$ two tailed.

Histopathology of Corneal Wounding

The average GHS of 63 corneas is provided in Table 2. As seen in Figure 6, a trend for the average GHS to increase throughout the culture period was observed.

Table 2. Average global histopathology scores (GHS) of 2 masked evaluators.

Cornea #	Treatment	Time in Culture	Pooled GHS		Cornea #	Treatment	Time in Culture	Pooled GHS
19-057	30s NaOH	0 hrs	3.5		19-070	30s NaOH	96hrs	6
19-065	60s NaOH	0 hrs	4.5		19-071	30s NaOH	96hrs	4.5
19-056	30s NaOH	24hrs	4		19-072	30s NaOH	96hrs	4.5
19-064	60s NaOH	24hrs	4		19-073	30s NaOH	96hrs	8
19-032	Blade	48hrs	3.5		19-074	30s NaOH	96hrs	8
19-055	30s NaOH	48hrs	5		19-075	30s NaOH	96hrs	9.5
19-063	60s NaOH	48hrs	8.5		19-076	30s NaOH	96hrs	9.5
19-029	Blade	72hrs	2.5		19-077	30s NaOH	96hrs	9
19-030	Blade	72hrs	4.5		19-078	30s NaOH	96hrs	9.5
19-089	15s NaOH	72hrs	10		19-079	30s NaOH	96hrs	10
19-090	15s NaOH	72hrs	9		19-080	30s NaOH	96hrs	10
19-097	15s NaOH	72hrs	4.5		19-081	30s NaOH	96hrs	11
19-098	15s NaOH	72hrs	2		19-082	30s NaOH	96hrs	11
19-054	30s NaOH	72hrs	6		19-061	60s NaOH	96hrs	6.5
19-083	30s NaOH	72hrs	10.5		19-045	30s HCl	120hrs	2
19-084	30s NaOH	72hrs	11		19-049	30s HCl	120hrs	2.5
19-085	30s NaOH	72hrs	9.5		19-046	60s HCl	120hrs	2
19-086	30s NaOH	72hrs	9.5		19-050	60s HCl	120hrs	3
19-087	30s NaOH	72hrs	10		19-043	30s NaOH	120hrs	3
19-088	30s NaOH	72hrs	10		19-047	30s NaOH	120hrs	1
19-062	60s NaOH	72hrs	7		19-052	30s NaOH	120hrs	8.5
19-099	2m N-Hep	72hrs	10		19-044	60s NaOH	120hrs	4
19-100	2m N-Hep	72hrs	10		19-048	60s NaOH	120hrs	6
19-101	2m N-Hep	72hrs	7		19-060	60s NaOH	120hrs	11
19-102	2m N-Hep	72hrs	9		19-025	Blade	144hrs	4
19-104	2m N-Hep	72hrs	6		19-026	Blade	144hrs	4
19-105	2m N-Hep	72hrs	8.5		19-027	Blade	144hrs	3.5
19-106	2m N-Hep	72hrs	7.5		19-028	Blade	144hrs	3
19-053	30s NaOH	96hrs	8.5		19-031	Blade	144hrs	4
19-067	30s NaOH	96hrs	10.5		19-051	30s NaOH	144hrs	9.5
19-068	30s NaOH	96hrs	9		19-059	60s NaOH	144hrs	11
19-069	30s NaOH	96hrs	6					

Figure 6

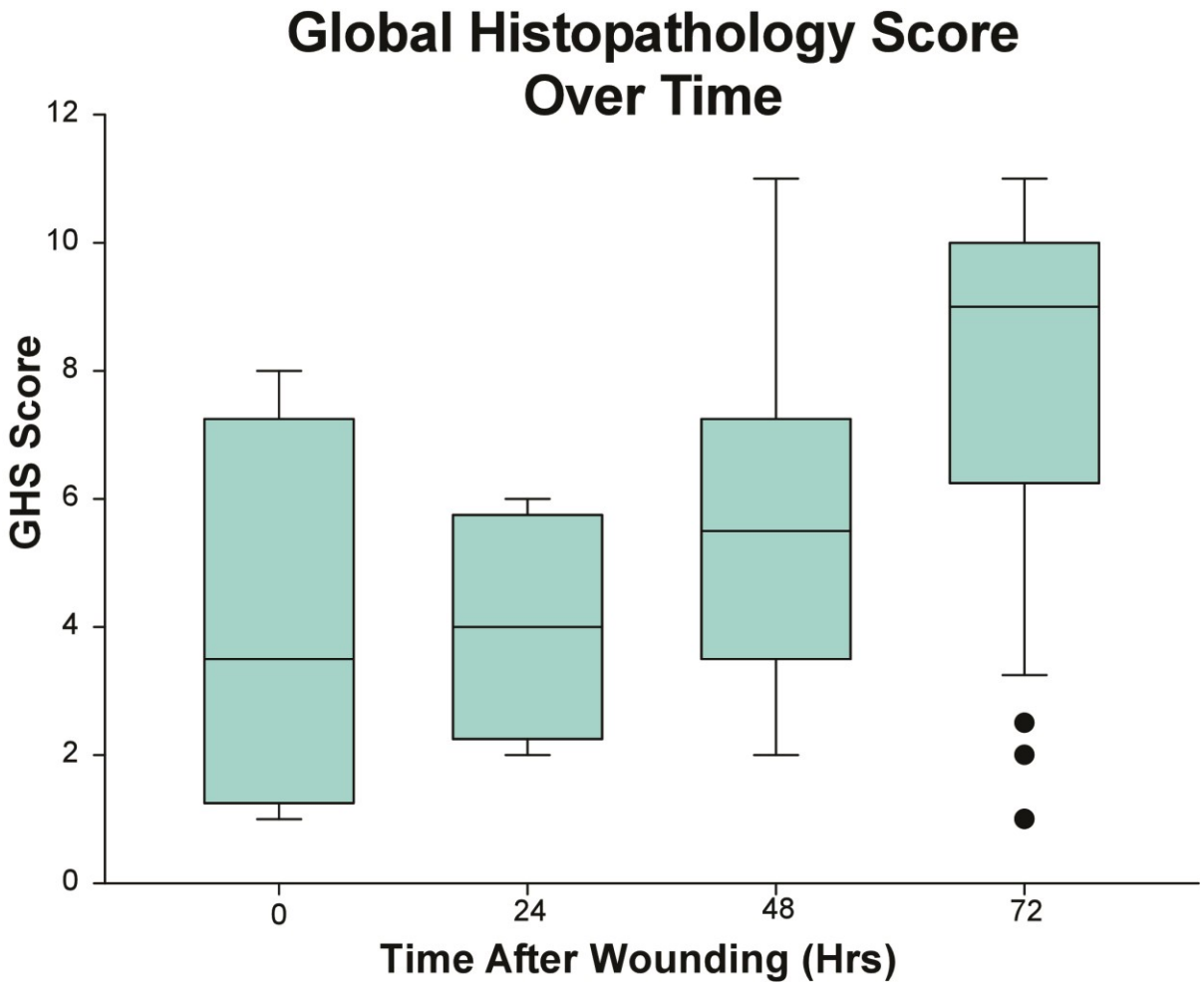

Figure 6. Global Histopathology Scores (GHS) vs time in culture. Note that the GHS average scores tended to increase over time.

Discussion

Here, we developed a cadaveric porcine corneal culture model system and used it to evaluate chemical and physical wounding methods and a novel method to evaluate fluorescein staining using 134 eyes. We cultured cadaveric porcine corneas for up to 96 hours and compared blade injury, and sodium hydroxide, hydrochloric acid, and N-heptanol chemical injuries in pilot work. Sodium hydroxide produced the most consistent injury here. We used two methods to assess the wound area by measuring fluorescein uptake. Both ImageJ Color Threshold and SpectraMax i3 were successful at assessing decreases in fluorescein-stained area over time which was consistent with wound healing. In contrast, histopathological appraisal did not show evidence of wound healing, perhaps since new epithelial cells were not assessed. The method described here provides a framework for culture, wounding and assessing cadaveric porcine cornea. We found decreases in the fluorescein-stained area which was taken as evidence of cornea wound healing. Since the Food and Drug Administration uses fluorescein staining for assessing efficacy in novel therapeutics [13], our work shows promise as a platform for drug testing in the future.

Our first goal was to establish a reliable method of 5 - 7 days cadaveric porcine corneal culture. This timeframe was selected because previous work indicated that significant wound healing occurs in within this time *in vitro* in rabbit [30], mouse [1] and swine models [25]. We also realized that full thickness remodeling of the wound is unlikely to occur *in vitro* since it requires 3-4 weeks *in vivo* [1,37]. Here, we defined "healing" as the primary closure akin to healing of first intent, where basal epithelial cells slide across and cover the wound, but tight junctions may not have been formed. Therefore, we aimed to develop a corneal culture system for the excised

cornea and limbal rim which permitted analysis over 72 – 96 hours consistently. We found that this was sufficient time for superficial wound closure to be documented using fluorescein staining.

We were not successful in maintaining the corneal cultures for over 96 hours (data not shown). Others have reported similar problems maintaining *in vitro* corneal cultures beyond 96 hours [17,28]. Our findings are consistent with the deterioration of corneal surface epithelium after 24 hours and the onset of tissue putrefaction after 48 hours as reported by Nioi et al. (2018) [38].

In contrast to our report and those discussed above, other laboratories-maintained corneas in vitro for > 30 days [18,19]. One possible explanation of these differences is the medium formulation used. The porcine cornea media used here is similar to previously described formulations [16-20,22,23,28,39], and this is unlikely to account for the differences. Second, the culture medium dispersal by orbital rocking of the plate may affect the cornea. This method was advocated previously [10-13], and it seems unlikely to contribute to differences observed. Third, contamination possibly triggering rapid degradation. Bacterial contamination was not likely the cause of culture failure here since the culture media contained antibiotics and antimycotics and was found to be free from bacteria. In summary, none of the above seem to reconcile the differences in culture viability with what was reported.

When we consider the physiologic requirements of the limbal rim, some explanations for the differences in culture are suggested. The porcine scleral thickness near the limbus is estimated to be 1.12 +/- 0.23 mm [40], while the adult human scleral thickness is approximately 0.5 mm [40]. Perhaps diffusion limitations of nutrients or oxygen might contribute to degradation over the 5 days observed here. The cornea is avascular and receives nutrition by diffusion through the aqueous humor [40], this supply was interrupted by culture and we assume the medium provide

suitable replacement. The cornea to sclera junction houses the limbal stem cells niche and has a high density of capillaries [41]. In future work, we suggest dissecting the deep surface of the limbus to minimize oxygen and nutrients diffusion distance to see if that permits longer culture. Unfortunately, investigating this matter further is beyond the scope of this report. In summary, for the purposes employed here, i.e., to evaluate corneal wounding and wound healing in a preclinical format, the methods described here demonstrated consistent wounding and wound healing over the 5-day culture period.

Our second goal was to evaluate *in vitro* corneal wounding methods considering there is no consensus or gold-standard method. Physical injury was investigated first because it seemed the simplest and clinically relevant. However, it was both slower and less consistent compared to the chemical methods. Chemical methods, including acidic, basic and n-Heptanol, were tested in pilot work (see supplemental materials) and 0.5N NaOH contact for 30 seconds was a good balance of wound depth and consistency. Lye (NaOH) injuries are fairly common and quite devastating injuries [26]. Slow epithelialization and persistent ulceration are some of the well-known complications of 2.0N NaOH in the acute phase of a corneal chemical burn [42]. In the case of the corneal wounds we investigated, 30-second application of 0.5N NaOH on a 7.2mm filter disk produced a visible area of corneal opacity in the cornea immediately (see Figure 2). There was a uniform degree of fluorescein stain uptake in the treated area, with a slow and consistent decline in the fluorescein-stained area over time. This is evidence of healing over 72 h of culture. Consistent with our findings, others showed that 2.0N NaOH resulted in corneal ulceration that progressed rapidly to deep ulceration and descemetocele [43] and that increasing the length of application or concentration of NaOH, significantly increases healing time [29]. In another *in vitro* study using cadaveric porcine eyeballs with 10 mm wounds using 2.0N NaOH for 20 seconds

showed the rapid denuding of the corneal epithelium and the swift accumulation of edema in the corneal stroma [26]. In summary, the results we obtained using 0.5N NaOH for 30 seconds fits with published cornea wound methods and produced a consistent wound.

Our third goal was to develop methods to assess wound healing. We used fluorescein-stained area to document the extent of cornea wounds, and we assumed that decreases in stained area corresponds with wound healing, knowing that full thickness cornea wound healing is likely to require 3-4 week *in vivo* [1,2]. We assumed that a decrease in the fluorescein-stained area within the cornea, and specifically in the region damaged at an earlier time point, would indicate "wound healing", but we did not independently validate that wound healing occurred. We used several methods to measure the area of fluorescein staining. First, we employed ImageJ-assisted photogrammetric assessment using ImageJ Color Threshold and ImageJ Outline methods. These methods rely on subjective determinations of the wound to set the capture area. Next, to reduce the subjective nature of the ImageJ techniques, we developed a plate reader-based fluorescence intensity method using a SpectraMax i3 spectrophotometer. Based upon these measures we conclude that significant wound healing was found using ImageJ Color Threshold and the SpectraMax i3 methods. The ImageJ Outline did not find significant wound healing. It is possible that some other mechanism contributed to decreased stained area over time. In fact, using histopathology to assess the wounded area suggested the opposite—that histopathology measured tissue damage trended in the opposite direction. Therefore, future work will be necessary to validate that wound healing was measured here, and not non-specific decreases in stained area.

The damage to the cornea was measured indirectly based upon fluorescein uptake. The mechanism of fluorescein uptake by damaged cornea epithelium is by direct transcellular

diffusion manifested whenever there is cell death or disruption of cell–cell junctions leading to paracellular spread [10,44,45]. Fluorescein staining is a well-established method and has been used to clinically assess cornea damage for more than 100 years. Furthermore, the Food and Drug Administration uses fluorescein staining for efficacy outcomes measures when evaluating new drugs [13]. For that reason, it was employed here.

The SpectraMax measures staining intensity in relative fluorescence units (RFUs). These non-standard units cannot be referenced back to a known luminosity. This is a limitation of our study. We attempted to generate a reference by adding known concentrations of fluorescein to establish a standard curve in well plates (data not shown). We were unable to standardize readings across days to establish a reference for use. In future work, we suggest that a reference phantom, perhaps by encapsulating fluorescein within transparent silicone, could be added to plates prior measurements. Perhaps by this method, a reference standard can be generated to replace RFUs and Z-scaling. Alternatively, a customized plate reader with programmable and referenced photomultiplier tube gain could be constructed to enable further testing of this assessment system. In contrast to the novel SpectraMax method we developed, other researchers have employed ImageJ for assessment successfully of corneal wounds [31], as we did here, and a second laboratory used 2D photogrammetry of fluorescein-stained corneas [28], consistent with our work. Therefore, in summary, there is previous work that supports our wound assessment methods using ImageJ. The consistency of the results between the ImageJ Threshold method and our SpectraMax results provides confidence that the plate reader method might be an innovation worth confirming and refining in future iterations.

We showed that both 2D photogrammetry and spectrophotometric methods show a trend toward decreased fluorescein-stained area, which we called healing, in both injury models over a

48 – 72-hour time period. The spectrophotometric method showed a larger effect size than ImageJ Color Threshold method. This observation will require additional follow-on work to confirm.

In regard to applying our methods for testing novel therapeutics, here are some considerations. First, our method evaluated fluorescein retention in 24-hour epochs. This may be too coarse readings to assess changes in wound healing induced by therapeutics. In this regard, validation and refinement of the SpectraMax method is important prior to extension in the drug testing. Because SpectraMax provides both staining intensity and area, it may provide more complex information about wound healing than the Color Threshold method, and perhaps a statistic that integrates both area and intensity can be calculated. This refinement will be required in follow-on work to compliment and extend the work described here.

One unexpected issue identified here was that histopathology findings did not follow the results obtained using other methods. Our method of histopathological evaluation was based on transverse sections that allowed the evaluation of all planes of the intact cornea – epithelium, basement membrane, and stroma. In contrast, our photographic and spectrophotometric methods appraised the fluorescein-stained area. Additionally, the 10 μm corneal sections were intended to be taken from the center of the wound and the selection of that location during slide preparation may have been off-target leading to an imprecise evaluation. In the future, accurate measures of the central corneal area will be needed for GHS analysis. This will involve sections taken from the central corneal region of each cornea and the most representative section selected for further analysis of healing.

A second unexpected issue was that the control, undamaged cornea had fluorescein staining at 0 hour that gradually increased (see Figure 5A) or gradually decreased (see Figure

5B). In gross observation the cornea became less glistening and more textured over 72 hours of culture (see Figure 2E). It has been hypothesized that normal corneas show sparse, scattered, punctate fluorescein uptake due to a time-dependent graded loss of the corneal glycocalyx, permitting transcellular entry into normally pre-shed cells [10]. The corneas used in controls experiments were lissamine-negative at time 0 and we assume that they were undamaged. However, the globes were transported *en masse* to the laboratory in cold PBS and the unprotected corneal surface may have been damaged. Therefore, the physical abrasion of the corneal surface during transport may be the cause of fluorescein staining. Perhaps it would be better to close the eyelids prior to transport, as done by others [31]. Another potential cause is disinfection of the eyes with 0.75% povidone iodine for 2 minutes. Perhaps this caused surface deterioration. Note that this concentration and contact time is used in both eye surgery and *in vitro* corneal research with no reported damage or increase in stain uptake following use [46,47]. Future directions to investigate staining of the uninjured control corneas include modification of the harvest procedure to include the eyelids with the adnexa of the eyeball and closing the eyelids prior to transport to minimize trauma.

Conclusion

In conclusion, my research addresses the strengths and limitations of an *in vitro* cadaveric porcine corneal wound model. We maintained corneas for 4 days in culture and produced predictable corneal wounding by NaOH exposure. We assessed wounds using ImageJ and a novel spectrophotometric-based method. Using an indirect measure based upon fluorescein-stained area, we found evidence of wound healing; however, further confirmation and refinement will be needed if one wishes to use to adopt this method for testing novel therapeutics.

Bibliography

1. Park M, Richardson A, Pandzic E, et al. Visualizing the contribution of Keratin-14(+) limbal epithelial precursors in corneal wound healing. *Stem Cell Rep* 2019;12:14-28.

2. Ljubimov AV, Saghizadeh M. Progress in corneal wound healing. *Prog Retin Eye Res* 2015;49:17-45.

3. Sridhar MS. Anatomy of cornea and ocular surface. *Indian J Ophthalmol* 2018;66:190-194.

4. Wipperman JL, MD, John N. Dorsch M. Evaluation and management of corneal abrasions. *Am Fam Physician* 2013;87:114-120.

5. Swain T, McGwin G, Jr. The prevalence of eye injury in the United States, estimates from a meta-analysis. *Ophthalmic Epidemiol* 2020;27:186-193.

6. Barrientez B, Nicholas SE, Whelchel A, et al. Corneal injury: Clinical and molecular aspects. *Exp Eye Res* 2019;186:107709.

7. Alario AF, Pirie CG. A spectral-domain optical coherence tomography device provides reliable corneal pachymetry measurements in canine eyes. *Vet Rec* 2013;172:605.

8. Paunksnis A, Svaldenienė E, Paunksnienė M, et al. Ultrasonographic evaluation of the eye parameters in dogs of different age. *ULTRAGARSAS* 2001;2:4.

9. Pantalon A, Pfister M, Aranha Dos Santos V, et al. Ultrahigh-resolution anterior segment optical coherence tomography for analysis of corneal microarchitecture during wound healing. *Acta Ophthalmol* 2019;97:e761-e771.

10. Bron AJ, Argueso P, Irkec M, et al. Clinical staining of the ocular surface: mechanisms and interpretations. *Prog Retin Eye Res* 2015;44:36-61.

11. Joyce PD. Corneal vital staining. *Irish J Med Sci* 1967;42:359-367.

12. De Schweinitz G. *Diseases of the Eye: A Handbook of Ophthalmic Practices for Students and Practitioners*. 10th ed: W.B. Saunders, 1924.

13. Begley C, Caffery B, Chalmers R, et al. Review and analysis of grading scales for ocular surface staining. *Ocul Surf* 2019;17:208-220.

14. Nishida T, Nakamura M, Ofuji K, et al. Synergistic effects of Substance P with Insulin-like Growth Factor-1 on epithelial migration of the cornea. *J Cell Physiol* 1996;169:159-166.

15. Colwell RN. *History and place of photographic interpretation, Manual of Photographic interpretation*. Bethesda: American Society for Photogrammetry & Remote Sensing, 1997.

16. Chan KY, Cho P, Boost M. Corneal epithelial cell viability of an ex vivo porcine eye model. *Clin Exp Optom* 2014;97:337-340.

17. Chuck RS, Beherns A, Wellik S, et al. Simple organ cornea culture model for re-epithelization after in vitro excitimer laser ablation. *Laser Surg Med* 2001;29:288-292.

18. Deshpande P, Ortega I, Sefat F, et al. Rocking media over ex vivo corneas improves this model and allows the study of the effect of proinflammatory cytokines on wound healing. *Investig Ophthal Vis Sci* 2015; 56: 1554-1561.

19. Harman RM, Bussche L, Ledbetter EC, et al. Establishment and characterization of an air-liquid canine corneal organ culture model to study acute herpes keratitis. *J Virol* 2014;88:13669-13677.

20. Wehrman RF. A novel ex vivo model of equine corneal wound healing. *Veterinary Clinical Sciences (Veterinary Medicine)*: Iowa State University, 2017.

21. Prinsen MK, Hendriksen CFM, Krul CAM, et al. The isolated chicken eye test to replace the draize test in rabbits. *Regul Toxicol Pharmacol* 2017;85:132-149.

22. Smeringaiova I, Reinstein Merjava S, Stranak Z, et al. Endothelial Wound Repair of the Organ-Cultured Porcine Corneas. *Curr Eye Res* 2018;43:856-865.

23. Zhao B, Cooper LJ, Brahma A, et al. Development of a three-dimensional organ culture model for corneal wound healing and corneal transplantation. *Investig Ophthalmol Vis Sci* 2006;47:2840-2846.

24. Zagon IS, Sassani JW, McLaughlin PJ. Re-epithelialization of the rabbit cornea is regulated by opioid growth factor. *Brain Res* 1998; 803:61-68.

25. Tappeiner C, Flueckiger F, Boehnke M, et al. Effect of topical anesthetic agents and ethanol on corneoepithelial wound healing in an ex vivo whole-globe porcine model. *J Cataract Refract Surg* 2012;38:519-524.

26. Rihawi S, Frentz M, Becker J, et al. The consequences of delayed intervention when treating chemical eye burns. *Graefes Arch Clin Exp Ophthalmol* 2007;245:1507-1513.

27. Maurer JK, Parker RD, Jester JV. Extent of initial corneal injury as the mechanistic basis for ocular irritation: key findings and recommendations for the development of alternative assays. *Regul Toxicol Pharmacol* 2002;36:106-117.

28. Chuck RS, Behrens A, Wellik S, et al. Re-epithelialization in cornea organ culture after chemical burns and excimer laser treatment. *Arch Ophthalmol* 2001;119:1637-1642.

29. Salman IA, Gundogdu C. Epithelial healing in experimental corneal alkali wounds with nondiluted autologous serum eye drops. *Cutan Ocul Toxicol* 2010;29:116-121.

30. Berta A, Holly FJ, Tozser J, et al. Tear plasminogen activators - indicators of epithelial cell destruction. The effect of scraping, n-heptanol debridement, and alkali burn of the cornea on the plasminogen activator activity of rabbit tears. *Int Ophthalmol* 1991;15:363-369.

31. Proietto LR, Whitley RD, Brooks DE, et al. Development and assessment of a novel canine ex vivo corneal model. *Curr Eye Res* 2017;42:813-821.

32. Kirazowa T, Kinoshira S, Fujira K, et al. The mechanism of accelerated corneal epithelial healing by human epidermal growth factor. *Investig Ophthal Vis Sci* 1990; 31:1773-1778.

33. Kim J, Foulks G. Evaluation of the effect of lissamine green and rose bengal on human corneal epithelial cells. *Cornea* 1999;18:328-332.

34. Pels E, Vrensen G. Microbial decontamination of human donor eyes with povidone-iodine: penetration, toxicity, and effectiveness. *Br J Ophthalmol* 1999; 83:1019-1026.

35. Schneider CA, Rasband WS, Eliceiri KW. NIH image to ImageJ: 25 years of image analysis. *Nat Methods* 2012;9.

36. Altmann S, Emanuel A, Toomey M, et al. A quantitative rabbit model of vaccinia keratitis. *Invest Ophthalmol Vis Sci* 2010;51:4531-4540.

37. Ljubimov AV. Diabetic complications in the cornea. *Vision Res* 2017;139:138-152.

38. Nioi M, Napoli PE, Demontis R, et al. Morphological analysis of corneal findings modifications after death: A preliminary OCT study on an animal model. *Exp Eye Res* 2018;169:20-27.

39. Oh JY. Procesing Porcine Cornea for Biomedical Applications. *Tissue Eng Part C* 2009;15:635-645.

40. Olsen TW, Sanderson S, Feng X, et al. Porcine sclera: thickness and surface area. *Investig Ophthal Vis Sci* 2002;43.

41. Grulkowski I, Liu JJ, Baumann B, et al. Imaging limbal and scleral vasculature using swept source optical coherence tomography. *Photonics Lett Pol* 2011;3:132-134.

42. Yao L, Li ZR, Su WR, et al. Role of mesenchymal stem cells on cornea wound healing induced by acute alkali burn. *PLoS One* 2012;7:e30842.

43. He J, Bazan NG, Bazan HEP. Alkali-induced corneal stromal melting prevention by a novel platelet-activating factor receptor antagonist. *Arch Ophthalmol* 2006;124.

44. Kim J. The use of vital dyes in corneal disease. *Curr Opin Ophthal* 2000;11:241-247.

45. Wilson G, Ren H, Laurent J. Corneal epithelial fluorescein staining. *J Am Optom Assoc* 1995;66:435-441.

46. Ferguson AW, Scott JA, McGavigan J, et al. Comparison of 5% povidone-iodine solution against 1% povidone-iodine solution in preoperative cataract surgery antisepsis: a prospective randomised double blind study. *Brit J Ophthalmol* 2003; 87.

47. Laubichler P, Arend N, Vounotrypidis E, et al. Comparing different decontamination procedures in harvesting human donor cornea. *Curr Eye Res* 2016;41:1173-1177.

Appendix A - Supplemental Material

2N Hydrochloric Acid Injury: A 7.2mm diameter (41mm^2) corneal wound was created by placing a filter disk saturated with 2N HCl on the cornea for either 30 or 60 s. Following HCl exposure the wounded surface was fluorescein-stained. There was little gross damage to the corneas immediately after wounding. The corneas were excised and placed on silicone supports in 6-well plates, covered with optical tape and imaged with the SpectraMax i3. After imaging, the optical tape was replaced with plates lids inside the biological safety cabinet and the plate was placed on the rotating platform within the incubator. Two corneas were exposed for 30 seconds and 2 were exposed for 60seconds (**see Figure 1S**). Variability in wound size was noted and we decided to not pursue HCl for corneal wounding.

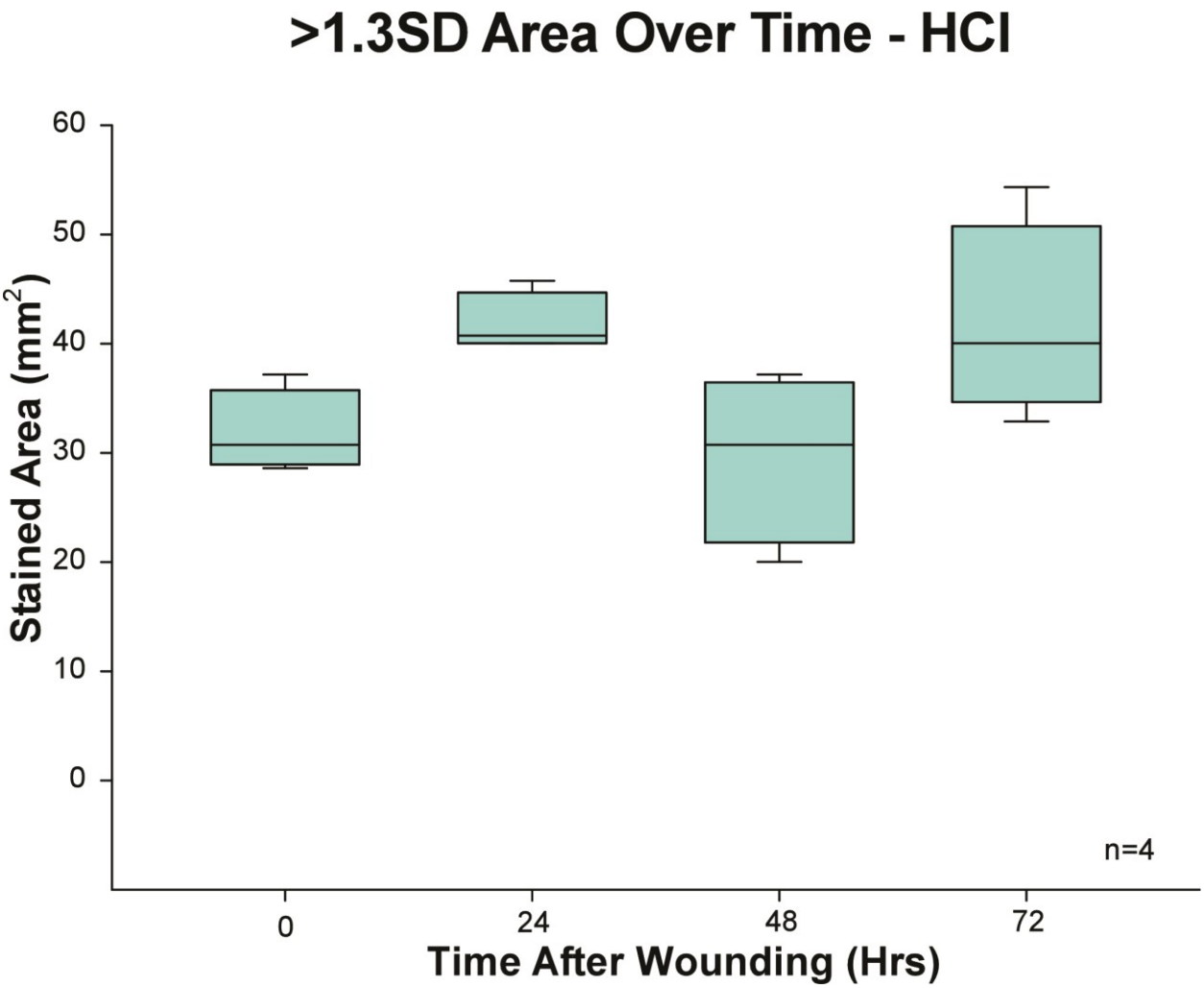

Figure 1S Fluorescein staining measured with SpectraMax i3 after hydrochloric acid (HCl) exposure. Following 60-second exposure of 2.0N HCl, no consistent changes in the fluorescein-stained area was seen over a 72-hour post-wound culture period.

99% N-Heptanol Injury: A 7.2mm diameter (41mm2) central corneal wound was made by placing a filter disk saturated with N-Heptanol as described in the Methods. 30- and 60 second and 2-minute exposure to N-Heptanol were investigated. Following N-Heptanol exposure the wounded surface was fluorescein-stained. After staining, the corneas were dissected and placed on silicone supports mounted in 6-well plates, covered with optical tape and imaged with the SpectraMax i3. After imaging, the optical tape was replaced with plates lids inside the biological safety cabinet and the plate was placed on the rotating platform within the incubator.

Following the N-Heptanol wounding, no gross damage was seen and diffuse fluorescein stain uptake. N-Heptanol resulted in erratic results (see figure 2S). Variability in wounding was noted and we decided to not pursue N-Heptanol for corneal wounding.

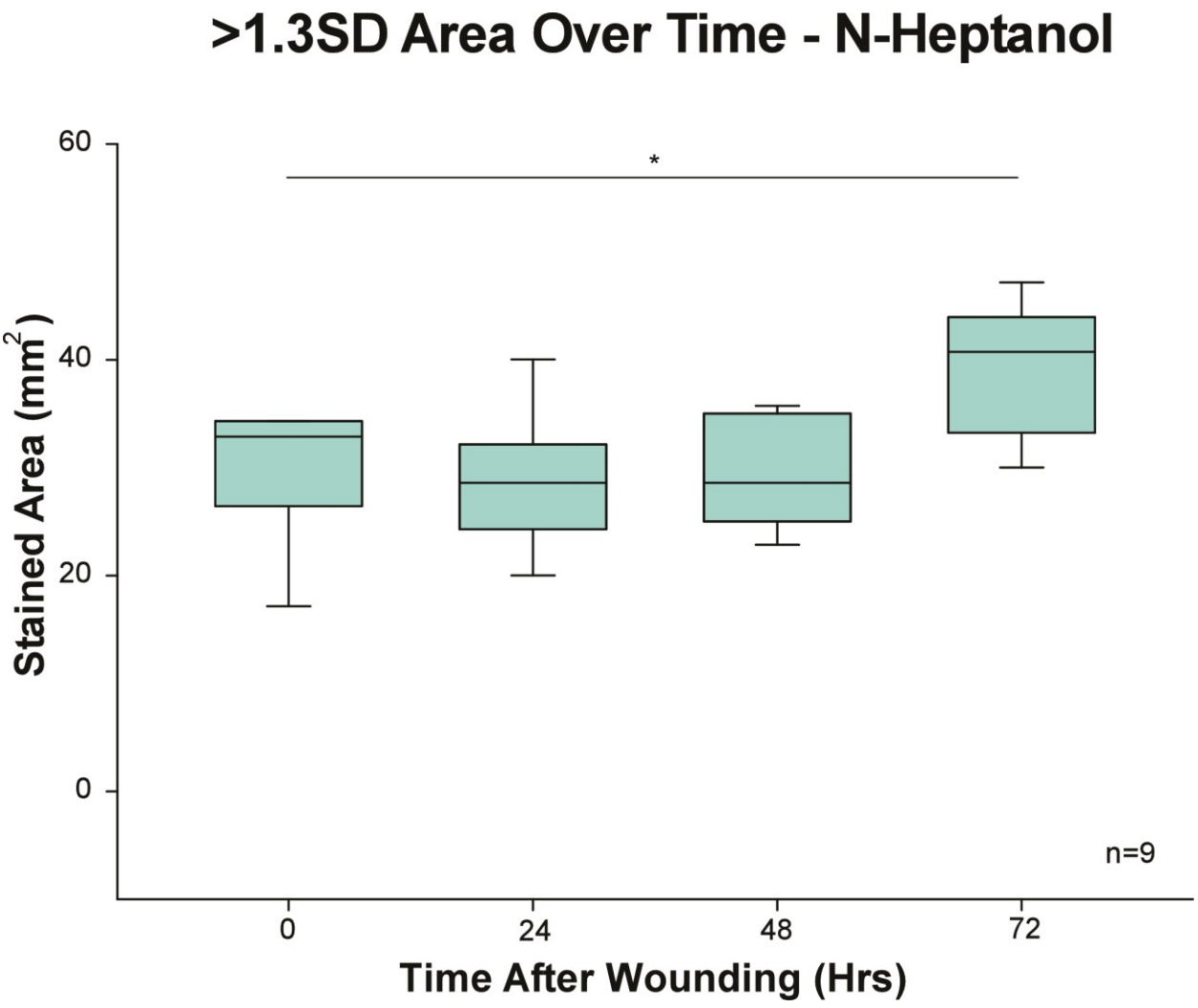

Figure 2S**.** Fluorescein staining measured with SpectraMax i3 after N-Heptanol exposure. Following a 2-minute exposure of 99% N-Heptanol no consistent changes in the fluorescein-stained area was seen over a 72-hour post-wound culture period.

Discussion of Supplementary Materials-

Chemically induced corneal wounds were investigated using 2N HCl, 0.5N NaOH and 99% N-Heptanol as described in the Methods. Acid exposure using HCl for 30 or 60 seconds

produced a chemical burn that was inconsistent, and this method of wounding was not pursued. Next, N-Heptanol was investigated since corneal ulceration was previously reported [21]. Here, thirteen corneas were tested with N-Heptanol with 30-s, 60-s or 2-min exposure. N-Heptanol was found to be inconsistent, and we discontinued testing.